Preprints of the 21st IFAC World Congress (Virtual)
Berlin, Germany, July 12-17, 2020

An Extremum Seeking Control Based Approach for Alignment Problem of Mobile Optical Communication Systems ⋆

Wenqi Cai * **Abdullah N. Alhashim** * **Ibrahima N'Doye** *
Taous Meriem Laleg-Kirati *

* *King Abdullah University of Science and Technology (KAUST), Thuwal 23955-6900, Saudi Arabia (e-mail: wenqi.cai@kaust.edu.sa, Abdullah.AlHashim@kaust.edu.sa, ibrahima.ndoye@kaust.edu.sa, taousmeriem.laleg@kaust.edu.sa)*

Abstract: Optical wireless communication (OWC) has proliferated a wide range of applications in many fields due to its advantages of low-cost, high bandwidth, etc. However, the strict alignment requirements of widely used line-of-sight (LOS) deployments are challenging to be achieved, especially for those moving optical communication systems. In this paper, we propose an extremum seeking control based control strategy to solve the alignment problem for mobile optical communication systems. Our proposed approach consists of two steps: coarse alignment and fine alignment, both rely on the measurements from the vision sensor Pixy2. The coarse alignment uses a feedback proportional-derivative (PD) control and is responsible for tracking and following the receiver. The objective of the fine alignment is to get rid of the effects of any static or dynamic disturbances. The perturbation-based extremum seeking control (ESC) is adopted for a continuous search for the optimal position, where the received optical power is maximum in the presence of disturbance. The proposed approach is simple, effective, and easy to implement.

Keywords: Mobile optical communication systems, beam alignment, extremum seeking control, tracking error, following error, PD, vision sensor.

1. INTRODUCTION

Optical wireless communication (OWC) is an emerging technology, which contains several categories: visible light communication (VLC), free space optical communication (FSO), underwater optical communication (UWOC), etc. In comparison to the radio frequency (RF) communication system, OWC provides several advantages (Uysal and Nouri (2014); Cai et al. (2019)). First, OWC systems operate in the unregulated spectrum, requiring no licensing fee, which provides a valuable opportunity for constructing low-cost OWC systems that help to alleviate the spectrum congestion currently evident in the 2.4GHz industrial, scientific, and medical (ISM) band (Jovicic et al. (2013)). Second, OWC systems have ultra-high bandwidth and are immune to electromagnetic interference. Furthermore, the high degree of spatial confinement brings OWC systems virtually unlimited reuse features, and the inherent physical security of OWC systems is also an important advantage over RF systems. With that, OWC technology has proliferated a wide range of applications in many fields.

However, in some applications like urban free space optical communication systems and optical communication-based autonomous underwater vehicle (AUV) systems, etc., the issue of pointing, acquisition, and tracking (PAT) (Gagliardi and Karp (1976)) impedes the developments of OWC. For achieving an energy-efficient and secure communication link, the narrow-beam based line-of-sight (LOS) configuration is usually employed in such systems, requiring strict alignment between the transmitter and the receiver (Baister and Gatenby (1994); Arnon (2010)). However, due to the disturbances (such as building sway-induced vibration, obstruction, ocean wave-induced instability, etc.) in the media environment, poly-directional movements of the transmitters, receivers, or base platforms, maintaining a LOS optical link is very difficult. And this is especially hard for the cases where both movements and disturbances exist, which usually refer to the mobile optical communication systems. The mobile and disturbing factors in the optical communication systems may impose the OWC system a large misalignment, which can lead to intolerable signal fading (Cai et al. (2018)). Hence, a very tight alignment system is required to reduce the power loss caused by misalignment between the transmitter and receiver.

Several methods have been proposed to address the alignment problem for optical communication systems. An interesting approach is to use multiple optical sources and multiple photodetectors (Simpson et al. (2012)) or photomultiplier tubes (Pontbriand et al. (2008)) to increase the active area of the transmitter and receiver. However, these multiple configurations will render high cost and high complexity for the system. Lee et al. (2000) presented a

⋆ This work has been supported by the King Abdullah University of Science and Technology (KAUST) Base Research Fund (BAS/1/1627-01-01) to Taous Meriem Laleg.

preliminary FSO pointing and tracking system by using a single focal plane array and a fine steering mirror; Amari et al. (2013) presented a beam tracking system based on a hybrid micro/nano manipulator and the Kalman filter (KF) algorithm. However, these methods are too complex and computationally expensive to be applied in mobile optical communication systems. Besides, a recent work (Solanki et al. (2018)) came up with an extended Kalman filter (EKF)-based tracking control, which exactly solves the alignment problem for the optical communication robot system. However, the EKF method requires the nonlinear model of the system, which is usually challenging to identify, and the adopted scanning motion causes considerable oscillations in the received optical power.

In this paper, we propose a new two-step control strategy to solve the alignment problem for image-based mobile optical communication systems. At first, we use the simple proportional-derivative (PD) control to accomplish the coarse alignment, including both tracking and following; and then the fine alignment is realized by using the extremum seeking control (ESC) algorithm, which helps to maintain tight alignment between transmitter and receiver and thus maximizes the received optical power. The proposed method is simple, effective, and easy to implement, and can achieve the highest communication quality even in the presence of varying disturbances.

The remainder of this paper is organized as follows. Section 2 introduces the experimental setup of the image-based mobile optical communication system. Then the proposed control approach is elaborately explained in sections 3 and 4, including PD and ESC, which correspond to coarse alignment and fine alignment respectively. The simulation results are given in section 5. Finally, conclusions and future work are provided in section 6.

2. EXPERIMENTAL SETUP

In this paper, we build an emulated mobile optical communication system, Fig. 1 shows the experimental setup. Two smart robot cars with drive motors are used as the moving platforms, which are controlled to move directionally by the Arduino UNO R3 microcomputers (Shenzhen XiaoR Geek Technology Co. (2018)); a laser and a photodiode are used as the transmitter and receiver, respectively. At the receiver side, the photodiode is directly mounted on the smart car. While at the transmitter side, the laser and vision sensor Pixy2 should be technically installed, as described below. The vision sensor (Pixycam (2019)), which is a camera that has vision processing capabilities, is mounted on a pan-tilt mechanism. The pan-tilt has two servo motors that rotate the Pixy2's yaw and pitch angles, and the rotation ranges are 130° and 90°, which are controlled by the Arduino UNO R3 as well. Besides, we use 3D printing to create a case where the laser can be mounted on top of Pixy2 so that laser and Pixy2 can move together wholly, as shown in the illustration. Therefore, with proper adjustment, the laser and photodiode can realize alignment when the camera is aligned with the receiver car (the two lines are parallel). In addition, it should be noted that the distance between the two cars can be obtained in real time by their radar sensors. The detailed parameters of these components are listed in Table 1.

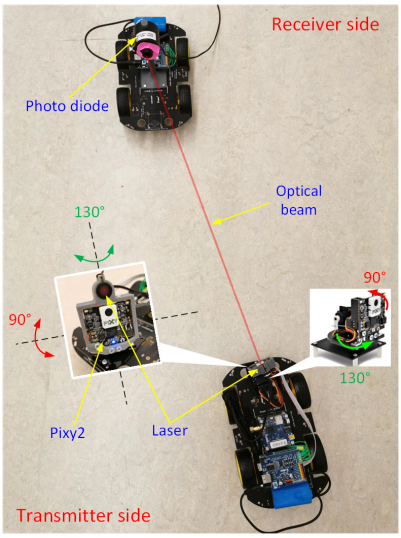

Fig. 1. Experimental setup of the image-based mobile optical communication system.

Table 1. Parameters of the image-based mobile optical communication system.

Description	Parameters	Value
Smart car	Model	Xiao-R robot
	Microcomputer	Arduino UNO R3
	Dimension	255 × 160 × 160mm
Laser	Distribution	Gaussian-like
	Wavelength	650nm
	Maximum power	5mW
Photo diode	Model	VLP-2000
	Maximum gain	20mW
	Resolution	0.001mW
	Effective aperture	10mm
Pixy2	Dimension	1.5 × 1.65 × 0.6in
	Image sensor	Aptina MT9M114
	Processor	NXP LPC4330
	Rotation angles	130° horizontal, 90° vertical

3. COARSE ALIGNMENT: FEEDBACK PD CONTROL

Our proposed method for the mobile optical communication system has two steps: coarse alignment and fine alignment, as shown in Fig. 2. The position coordinates of the receiver in the image frame (x, y) is the input of the system. For a tracking error (pan error or tilt error) or a following error (angle error or distance error), the feedback PD control is applied to eliminate these errors. Then, to get rid of the effects of any disturbances, a fine alignment using the perturbation-based ESC is adopted to keep finding the optimal position, which allows getting the maximum received optical power P_{max} at the receiver.

3.1 Tracking

The tracking control is realized by Pixy2 (Pixycam (2019)). Pixy2 is a color vision sensor, which means it recognizes objects by the specific color of each object. Before the recognition, we teach Pixy2 to "learn" (store) the color codes, in Fig. 3 for example, the color code is pink

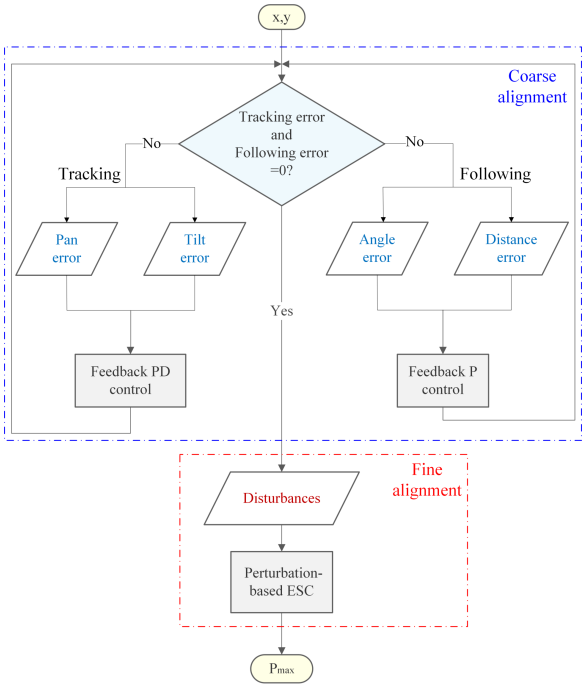

Fig. 2. Flow diagram of the proposed two-step control strategy

and yellow. It is worth noting that the stored color can be a combination of many colors, which ensures the accuracy of identification. There are two errors in the image, pan error and tilt error, which are the horizontal and vertical offsets of an object from the center (setpoint) of the image frame. The objective is to eliminate these errors so that the receiver is continuously kept at the center of the image frame, which means the transmitter keeps tracking the moving receiver.

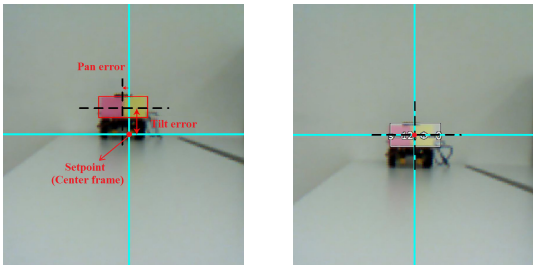

(a) Deviation (b) Center

Fig. 3. Tracking error illustration

When the receiver (color code) is recognized by Pixy2, a bounding box is drawn on it as shown in Fig. 3. This hard work of receiver detection and localization is handled by the image processing system inside the Pixy2 camera, and the position coordinates, block size, and color code of the detected receiver will be reported back to Arduino. In the Arduino, the information of position coordinates (x, y) is utilized to adjust the pan and tilt servos to keep the tracked receiver in the center of the image frame. The simple feedback PD control is used for both pan and tilt servos (Bill Earl (2014)),

$$\begin{aligned} u_i &= K_P e_i + K_D(e_i - e_{i-1}) \\ u_t &= \sum_{i=0}^{n} u_i, \end{aligned} \tag{1}$$

where K_P and K_D are the PD gains, e_i is the pan or tilt error, and u_t is the control input to the pan or tilt servo. It is worth noting that since we control how much the servos rotate, the control value u_i is added to the previous values. And pan and tilt servos control the angular velocity of the Pixy2 (laser transmitter).

3.2 Following

The following control is realized by the smart car. When following the receiver car, there will be two errors as well, namely angle error and distance error. Angle error refers to the angle between the connection line of transmitter-receiver and the moving direction of the transmitter car, as shown in Fig. 4. Distance error means the distance between the current position and the required fixed following distance, which depends on different communication systems (in the simulation part, we set the following distance as 1 meter). Therefore, when both errors are zero, the transmitter car directly faces the receiver car at a certain distance, and then Pixy2 is parallel to the front edge of the car.

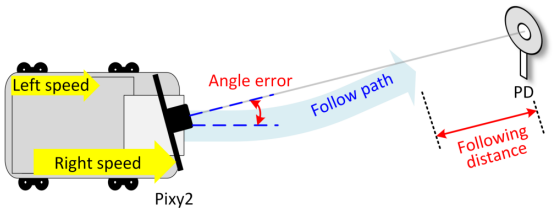

Fig. 4. Following error illustration

Similar to the tracking control, for the following control, the measurements of block size and position coordinates from the image of Pixy2 are reported to Arduino to adjust the left and right drive motors, which control the car to move toward the desired direction and keep a specific following distance. The position coordinates provide information on how far the car is turned away from the transmitter-receiver direction (how much is the angle error), which is used to control the speed difference between the left and right wheels, making the transmitter car to turn to the desired direction. To eliminate the distance error, we use the information of block size, which shows how far away the receiver is, and the value can be used to calculate the forward speed. For example, if the transmitter car is approaching the receiver, the transmitter car will slow down; if the block of the receiver appears larger than the set point value, the car will move backward. The simple feedback P control is used for both left and right drive motors (Bill Earl (2014)),

$$u_f = K_{P'} e_j, \tag{2}$$

where $K_{P'}$ is the controller gain, e_j is the angle error or distance error, and u_f is the control input to the left or right motor. The left and right motors control the linear velocity of the Pixy2 (laser transmitter).

4. FINE ALIGNMENT: EXTREMUM SEEKING CONTROL

With coarse alignment control, the transmitter (laser) is capable of following and tracking the receiver (photodiode). However, due to the existence of the system internal or external interference factors, although the error

of coarse alignment is zero, the receiver and transmitter might not be perfectly aligned. Therefore, our next step is to adopt the perturbation-based ESC, aiming at achieving the best alignment and obtaining the maximum received power. ESC is an optimal control strategy; it exactly matches our objective, which is to maximize the received optical power. Furthermore, the reasons why we adopt ESC rather than other optimal control methods are the following (Zhang and Ordóñez (2011)):

- Model-free property of ESC helps to avoid the complexity of building a system model.
- ESC could optimize the output without knowing the cost function, which means ESC controller only relies on the measurements of the cost function.
- ESC allows tracking an undetermined varying maximum of a cost function, which is very useful in the complicated and varying optical communication environments.

To evaluate the performance of the proposed ESC controller theoretically, we establish a dynamic model of the described system and design an ESC controller based on the model, which is introduced below.

4.1 Model Design

The classical image-based system has been best described with dynamic models. In this paper, we derive the image-based optical communication dynamic model based on the previous work Chaumette and Hutchinson (2006).

First, define two vectors for the system: $R = (X, Y, Z)$ is the coordinates for the receiver in the 3-D space; $I = (x, y)$ is the corresponding coordinates in the image frame, on which the receiver projects. Their relation can be expressed as (Forsyth and Ponce (2003); Ma et al. (2012))

$$\begin{cases} x = X/Z = (u - c_u)/f\alpha \\ y = Y/Z = (v - c_v)/f, \end{cases} \tag{3}$$

where u, v represent the coordinates of the image point expressed in pixel units, and c_u, c_v, f, α are the parameters of the camera itself: c_u, c_v are the coordinates of the principal point; f is the focal length; α is the ratio of the pixel dimensions.

Then, taking the derivative of (3) with respect to time, we have

$$\begin{cases} \dot{x} = \dot{X}/Z - X\dot{Z}/Z^2 = (\dot{X} - x\dot{Z})/Z \\ \dot{y} = \dot{Y}/Z - Y\dot{Z}/Z^2 = (\dot{Y} - y\dot{Z})/Z. \end{cases} \tag{4}$$

Now recall the below well-known equation (Forsyth and Ponce (2003); Ma et al. (2012))

$$\dot{R} = -v_r - \omega_r \times R, \tag{5}$$

where $v_r = [\, v_x \;\; v_y \;\; v_z \,]^{\mathrm{T}}$ is the linear velocity of the camera (Pixy2), $\omega_r = [\, \omega_x \;\; \omega_y \;\; \omega_z \,]^{\mathrm{T}}$ is the angular velocity of the camera (Pixy2), and '$\times$' represents the outer product. Specifically,

$$\dot{R} = \begin{bmatrix} \dot{X} \\ \dot{Y} \\ \dot{Z} \end{bmatrix} = \begin{bmatrix} -v_x - \omega_y Z + \omega_z Y \\ -v_y - \omega_z X + \omega_x Z \\ -v_z - \omega_x Y + \omega_y X \end{bmatrix}. \tag{6}$$

Then, relate the velocity of the camera (Pixy2) to the coordinates derivative of the receiver by substituting (6) into (4), we get (Chaumette and Hutchinson (2006))

$$\begin{cases} \dot{x} = -v_x/Z + xv_z/Z + xy\omega_x - (1 + x^2)\omega_y + y\omega_z \\ \dot{y} = -v_y/Z + yv_z/Z - xy\omega_y + (1 + y^2)\omega_x - x\omega_z. \end{cases} \tag{7}$$

As mentioned before, the distance of the receiver relative to the camera frame can be obtained in real time by the mounted radar sensors, so Z is known and fixed (following distance error is zero). Besides, in this work, we don't consider the vertical movement (y axis) of the smart car, and because Pixy2 only rotates around x, y axes, the system can be reduced to

$$\begin{bmatrix} \dot{x} \\ \dot{y} \end{bmatrix} = \begin{bmatrix} \frac{-1}{Z} & \frac{x}{Z} & xy & -(1 + x^2) \\ 0 & \frac{y}{Z} & (1 + y^2) & -xy \end{bmatrix} \begin{bmatrix} v_x \\ v_z \\ \omega_x \\ \omega_y \end{bmatrix}, \tag{8}$$

which is in the nonlinear form of

$$\dot{I} = A(I)U_c. \tag{9}$$

4.2 Controller Design

The objective now is to design a perturbation-based ESC controller based on the model derived above. Considering a new variable I_0 (which is unknown) and let

$$\tilde{I} = I - I_0 = \begin{bmatrix} x \\ y \end{bmatrix} - \begin{bmatrix} x_0 \\ y_0 \end{bmatrix}. \tag{10}$$

If so,

$$\dot{\tilde{I}} = \dot{I} = AU_c. \tag{11}$$

By using the feedback linearizing control

$$U_c = -cA^T\tilde{I}, \tag{12}$$

where c is a positive constant, 'T' represents the pseudo inverse, we could get

$$\dot{\tilde{I}} = -cAA^T\tilde{I} = -c\tilde{I} = -c\left(\begin{bmatrix} x \\ y \end{bmatrix} - \begin{bmatrix} x_0 \\ y_0 \end{bmatrix}\right). \tag{13}$$

Obviously, the system of (13) is exponentially stable with equilibrium point (x_0, y_0). If we let the reference position (x_0, y_0) to be the optimal position (x^*, y^*), the state (x, y) will reach the optimal position (x^*, y^*) exponentially. To do this, the perturbation-based ESC scheme shown in Fig. 5 is applied to adjust (x_0, y_0) to (x^*, y^*).

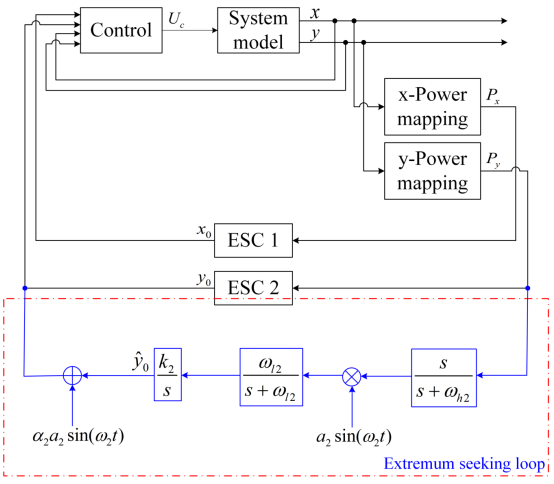

Fig. 5. Fine alignment via perturbation-based extremum seeking control.

4.3 Extremum Seeking Control

Figure 5 shows the system block diagram of fine alignment via ESC control, which is composed of four parts: controller, system model, power mapping, and ESC. Power mapping is the so-called cost function (performance function). The optical power distribution of the laser utilized in this work obeys Gaussian-like distribution. Therefore, the received optical power and position coordinates have a Gaussian-like relation, which means the mappings between P_x, P_y and x, y are concave functions. For simulation purpose, we postulate two simple mapping functions (Ariyur and Krstic (2003)) (approximate well in the neighborhood of the peak)

$$\begin{aligned} P_x &= 2(P_x)_{\max} \cdot \frac{x^* x}{(x^*)^2 + x^2}, \\ P_y &= 2(P_y)_{\max} \cdot \frac{y^* y}{(y^*)^2 + y^2}, \end{aligned} \tag{14}$$

where x^*, y^* are the optimal positions, $(P_x)_{max}, (P_y)_{max}$ are the maximum power, satisfying that $P_x = (P_x)_{max}$, $P_y = (P_y)_{max}$ if $x = x^*$, $y = y^*$ ($(P_x)_{max} = (P_y)_{max} =$ 5mW in this work).

The ESC process is illustrated in the dotted box (note that only the process of ESC 2 is shown because ESC 1 and ESC 2 have exactly the same structure; the only differences are the design parameters, which are distinguished by subscripts 1 and 2). For a more detailed explanation about the principles and the proof of asymptotic convergence of the perturbation-based ESC, please see Krstic and Wang (2000); Ariyur and Krstic (2003). Simply speaking, once we get the measurements of the received power P_x, P_y and input them to ESC, we will get an updated value of the reference position (x_0, y_0), which is tuned iteratively according to the power mapping function to reach the optimal position (x^*, y^*). Therefore, the position of the receiver (x, y) would also reach the optimal position (x^*, y^*). As can be seen, the difference between fine alignment and coarse alignment is that the "optimal position" for fine alignment is where the system can actually receive the maximum optical power, rather than the previous "center position". This ensures that fine alignment using ESC can find the best position to get the maximum optical power even in the presence of interference.

5. SIMULATION RESULTS

The coarse alignment uses simple feedback PD control and is already accomplished by the Arduino. Therefore, the simulation only focuses on the ESC part. We perform the simulation by SIMULINK using the same scheme in Fig. 5, in which ω_h is the cutoff frequency of the high pass filter, ω_l is the cutoff frequency of the low pass filter, k, α are some positive constants, and $asin(\omega(t))$ is the injected sinusoidal perturbation. The simulation parameters of the double-loop ESC are listed in Table 2. Note that the sinusoidal perturbation for each loop should has distinct frequency (i.e., $\omega_1 \neq \omega_2$) (Eleiwi and Laleg-Kirati (2018)), and the design parameters for each loop are also set independently until the whole process is tuned out to have the optimal result (Calli et al. (2012)). Besides, the choice of the frequencies should follow $\omega_h < \omega_l < \omega$ (Rotea (2000)). In the simulation, both ω and α are set to small enough values, so that the sinusoidal fluctuations on the control input have a lower frequency and a smaller amplitude, which is suitable for the fine alignment and is good for the actuator in practical application. In the following, we consider two simulation cases, static disturbance and dynamic disturbance.

Table 2. ESC design parameters.

ESC 1		ESC 2	
Parameters	Value	Parameters	Value
ω_1	3.2	ω_2	3.4
a_1	1	a_2	1
α_1	0.005	α_2	0.005
ω_{h1}	0.6	ω_{h2}	0.7
ω_{l1}	1.2	ω_{l2}	1.4
k_1	0.327	k_2	0.476

5.1 Static Disturbance

A static disturbance refers to the disturbance that renders a static error between the current position (x, y) (after the coarse alignment) and the optimal position (x^*, y^*). For example, something bumps into the car, causing that the two lines (Pixy2-receiver car and laser-photodiode) are no longer parallel, which means although the error of coarse alignment is zero, the laser and photodiode are actually not aligned. In the simulation, we assume the current position coordinate is $(x, y) = (5, 5)$, which is the center of the image frame. However, the optimal position after a static disturbance is $(x^*, y^*) = (2, 3)$.

The simulation results of ESC with static disturbance are shown in Fig. 6. As can be seen, the receiver's position coordinates (x, y) gradually reach the steady value of the reference position (x_0, y_0), i.e. decrease from (5,5) to (2,3). By applying the ESC controller, P_x and P_y gradually increase to the maximum of 5mW as expected; While without ESC controller, P_x and P_y keep at the constant values, which are lower than 5mW due to the misalignment caused by static disturbance. Besides, as mentioned earlier, because the selected parameters α, ω are small, the final fluctuations of the control inputs are very tiny, as shown in Fig. 6(c).

5.2 Dynamic Disturbance

A dynamic disturbance refers to the disturbance that varies with time, such as tiny ground vibration, so that the optimal position (x^*, y^*) is not a fixed value, but changes slightly all the time. However, ESC is able to track the unknown, varying optimal position, which provides solutions to more realistic problems. In the simulation, the current position coordinate is $(x, y) = (5, 5)$, and we introduce two varying disturbances to the system randomly, such that the variances of the disturbances for x axis and y axis are 0.2 and 0.1, respectively.

The simulation results of ESC with dynamic disturbance are shown in Fig. 7. Different from the last case, the value of (x, y), closely following the value of (x_0, y_0), keeps in

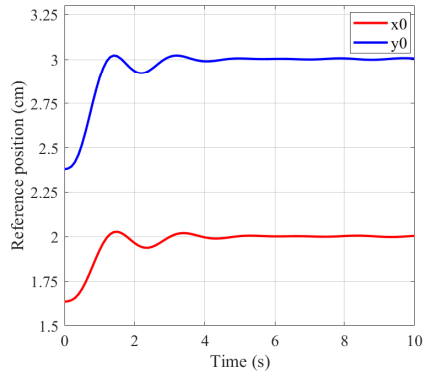

(a) Reference position

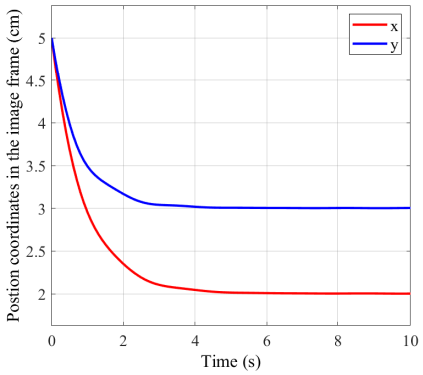

(b) Position coordinates

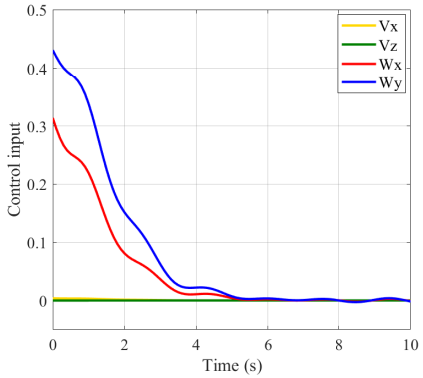

(c) Control input U_c

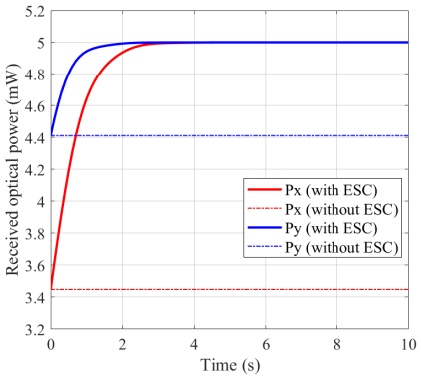

(d) Received optical power

Fig. 6. Simulation results of ESC with static disturbance

a slight change after gradually falling to the vicinity of $(2, 3)$. This can be observed from the data points marked in Fig. 7(a) and Fig. 7(b). In order to make (x, y) consistently follow the varying (x^*, y^*), the control inputs make small adjustments around zero as shown in Fig. 7(c), so as to keep the received optical power at 5mW as far as possible. Most importantly, compared with the case without ESC, after adopting the ESC controller, the received optical power P_x and P_y can not only significantly resist the effects of the dynamic disturbance but also keep the received power close to the maximum of 5mW. The simulation results in Fig. 7(d) prove that the designed ESC controller can realize fine alignment in spite of dynamic disturbance.

6. CONCLUSION

In this paper, an ESC-based two-step control strategy aims to solve the alignment problem for mobile optical communication systems has been presented. We use the simple feedback PD control and perturbation-based extremum seeking control for coarse alignment and fine alignment purposes. The simulation results show that ESC is an excellent choice for solving the optical alignment problem. From a practical point of view, our proposed method is simple, effective, and easy to implement, and can achieve the highest communication quality even in the presence of varying disturbances. Furthermore, although we only consider one specific scenario in this work, the proposed method could be extended to more extensive optical communication scenarios, such as a high-speed underwater optical communication system for AUV and seabed station. Our intention in the future is to do the real implementation and combine this method with other localization techniques, such as Kalman filter, to solve more complicated mobile optical communication alignment problems.

REFERENCES

Amari, N., Folio, D., and Ferreira, A. (2013). Robust laser beam tracking control using micro/nano dual-stage manipulators. In *2013 IEEE/RSJ International Conference on Intelligent Robots and Systems*, 1543–1548. IEEE.

Ariyur, K.B. and Krstic, M. (2003). *Real-time optimization by extremum-seeking control*. John Wiley & Sons.

Arnon, S. (2010). Underwater optical wireless communication network. *Optical Engineering*, 49(1), 015001.

Baister, G. and Gatenby, P. (1994). Pointing, acquisition and tracking for optical space communications. *Electronics and Communication Engineering Journal*, 6(6), 271–280.

Bill Earl (2014). *Pixy Pet Robot - Color vision follower*. Adafruit Industries.

Cai, W., N'Doye, I., Sun, X., Al-Awan, A., Alheadary, W.G., Alouini, M.S., Ooi, B., and Laleg-Kirati, T.M. (2018). Robust H_∞ pointing error control of free space optical communication systems. In *2018 IEEE Conference on Control Technology and Applications (CCTA)*, 958–963. IEEE.

Cai, W., N'Doye, I., Ooi, B.S., Alouini, M.S., and Laleg-Kirati, T.M. (2019). Modeling and experimental study of the vibration effects in urban free-space optical communication systems. *IEEE Photonics Journal*, 11(6), 1–13.

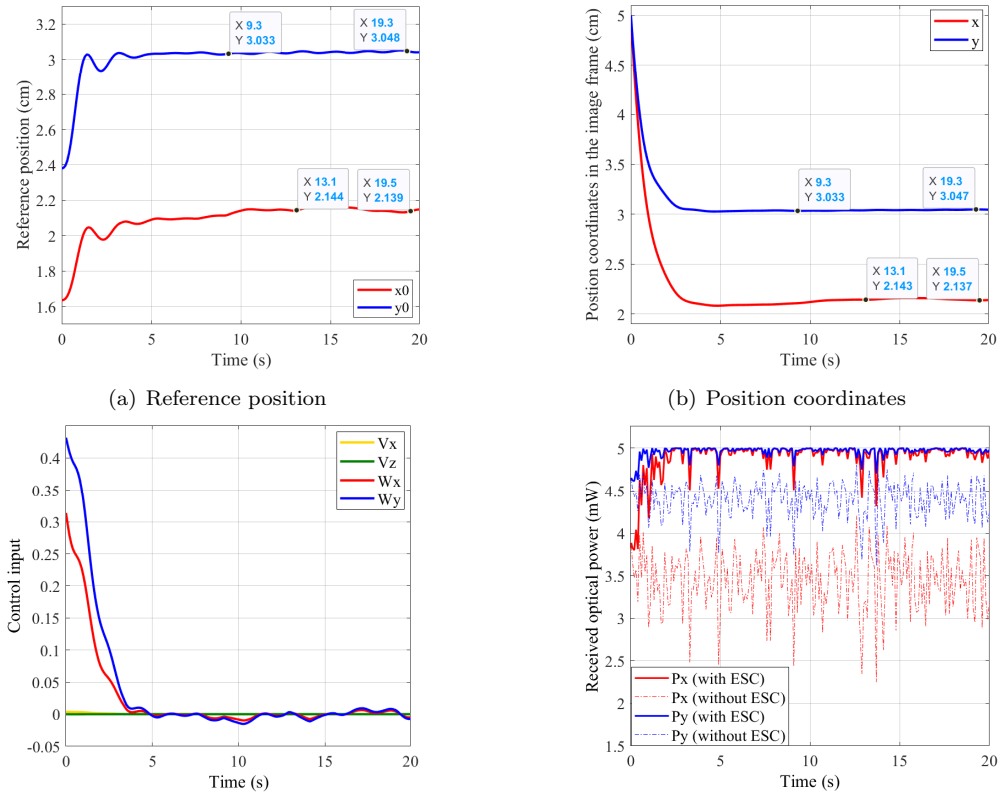

(a) Reference position

(b) Position coordinates

(c) Control input U_c

(d) Received optical power

Fig. 7. Simulation results of ESC with dynamic disturbance

Calli, B., Caarls, W., Jonker, P., and Wisse, M. (2012). Comparison of extremum seeking control algorithms for robotic applications. In *2012 IEEE/RSJ International Conference on Intelligent Robots and Systems*, 3195–3202. IEEE.

Chaumette, F. and Hutchinson, S. (2006). Visual servo control part I: Basic approaches. *IEEE Robotics Automation Magazine*, 13(4), 82–90.

Eleiwi, F. and Laleg-Kirati, T.M. (2018). Observer-based perturbation extremum seeking control with input constraints for direct-contact membrane distillation process. *International Journal of Control*, 91(6), 1363–1375.

Forsyth, D.A. and Ponce, J. (2003). *Computer vision: a modern approach*. Prentice-Hall.

Gagliardi, R.M. and Karp, S. (1976). Optical communications. *New York, Wiley-Interscience*, 445.

Jovicic, A., Li, J., and Richardson, T. (2013). Visible light communication: opportunities, challenges and the path to market. *IEEE Communications Magazine*, 51(12), 26–32.

Krstic, M. and Wang, H.H. (2000). Stability of extremum seeking feedback for general nonlinear dynamic systems. *Automatica*, 36(4), 595–601.

Lee, S., Alexander, J.W., and Jeganathan, M. (2000). Pointing and tracking subsystem design for optical communications link between the international space station and ground. In *Free-Space Laser Communication Technologies XII*, volume 3932, 150–157. International Society for Optics and Photonics.

Ma, Y., Soatto, S., Kosecka, J., and Sastry, S.S. (2012). *An invitation to 3-D vision: from images to geometric models*. Springer Science & Business Media.

Pixycam (2019). Pixy2 overview. `https://docs.pixycam.com/wiki/doku.php?id=wiki:v2:overview`.

Pontbriand, C., Farr, N., Ware, J., Preisig, J., and Popenoe, H. (2008). Diffuse high-bandwidth optical communications. In *OCEANS 2008*, 1–4. IEEE.

Rotea, M.A. (2000). Analysis of multivariable extremum seeking algorithms. In *Proceedings of the 2000 American Control Conference (ACC)*, volume 1, 433–437. IEEE.

Shenzhen XiaoR Geek Technology Co., L. (2018). Ds arduino uno wifi video car robot. `http://www.xiao-r.com/index.php/Study/catalog/cid/1`.

Simpson, J.A., Hughes, B.L., and Muth, J.F. (2012). Smart transmitters and receivers for underwater free-space optical communication. *IEEE Journal on selected areas in communications*, 30(5), 964–974.

Solanki, P.B., Al-Rubaiai, M., and Tan, X. (2018). Extended kalman filter-based active alignment control for led optical communication. *IEEE/ASME Transactions on Mechatronics*, 23(4), 1501–1511.

Uysal, M. and Nouri, H. (2014). Optical wireless communications—an emerging technology. In *2014 16th International Conference on Transparent Optical Networks (ICTON)*, 1–7. IEEE.

Zhang, C. and Ordóñez, R. (2011). *Extremum-seeking control and applications: a numerical optimization-based approach*. Springer Science & Business Media.